LA-UR- 99-2933

Approved for public release; distribution is unlimited.

Title:	Performance of Multi-Element CdZnTe Detectors
Author(s):	Calvin E. Moss (NIS-6) ✓ Kiril D. Ianakiev (NIS-5) ✓ Thomas H. Prettyman (NIS-5) ✓ Robert C. Reedy (NIS-2) ✓ Morag K. Smith (NIS-5) ✓ Martin R. Sweet (NIS-5) ✓ John Valentine (Georgia Institute of Technology)
Submitted to:	44th Annual Symposium on Optical Science Society of Optical Engineering 18-23 July 1999 Denver, Colorado

Performance of multi-element CdZnTe detectors

Calvin E. Moss*[a], Kiril D. Ianakiev[b], Thomas H. Prettyman[b], Robert C. Reedy[c], Morag K. Smith[b], Martin R. Sweet[b], John D. Valentine[d]

[a]Los Alamos National Laboratory, MS J562, Los Alamos, NM 87545
[b]Los Alamos National Laboratory, MS E540, Los Alamos, NM 87545
[c]Los Alamos National Laboratory, MS D436, Los Alamos, NM 87545
[d]Georgia Institute of Technology, George W. Woodruff School of Mechanical Engineering, Atlanta, GA 30332-0405

ABSTRACT

Single-element CdZnTe detectors are limited in size, and therefore efficiency, by the poor hole transport, even with a coplanar grid. We are investigating the possibility of a 27-element (3 × 3 × 3) array using 15 mm × 15 mm × 15 mm elements for gamma-ray energies to 10 MeV for NASA planetary missions. We present experimental results for combinations of various size coplanar grid detectors using NIM electronics and energies to 6.1 MeV. Summation of the signals after linear gating and requiring coincidence produces only a small increase in the energy resolution. Our results indicate that good efficiency and a spectrum not complicated by a large Compton continuum can be achieved by simply summing the spectra from 15 × 15 × 15 mm^3 detectors for gamma-ray energies below about 2 MeV. Above 2 MeV, 2-fold coincidence might be required, depending on the spectrum, to suppress the Compton continuum and escape peaks. We use a Monte Carlo calculation to predict the performance of the 27-element array for a lunar highlands spectrum. Such ambient-temperature, high-efficiency, good-resolution arrays will facilitate new NASA missions to determine elemental composition of planetary bodies and terrestrial applications requiring high-efficiency, good-resolution portable instruments.

Keywords: Cadmium Zinc Telluride, gamma-ray detector, radiation detector, detector array, planetary science

1. INTRODUCTION

1.1. Planetary science requirements

The determination of the chemical composition and its variation across the surface of a planetary body is fundamental in understanding the formation and evolution of that body. Measurement of the gamma-ray line emissions from materials is a well-established technique for determining elemental composition. Gamma-ray emissions from planetary bodies are mainly from the naturally radioactive nuclides Th, U, K and their daughters and from reactions of primary and secondary cosmic rays particles with other nuclides. The primary cosmic rays can cause spallation reactions that produce neutrons. The fast neutrons can cause inelastic scattering reactions, (n,n'γ). The neutrons can also be moderated to thermal energies and cause capture reactions, (n,γ). Such reactions produce characteristic gamma-ray lines from almost all elements, but the ones from reactions on H, O, Si, Al, Mg, Fe, Ti, and Ca are of most interest for studying planetary bodies. Figure 1 shows a calculation of the gamma-ray lines expected from Mars. Analyses of measured spectra yield an average composition to a depth of a few tens of centimeters, the range of gamma rays in materials, thus complementing analyses with x rays, UV, visible, and IR emissions, which have much shorter ranges.

Gamma-ray measurements can be performed from orbit or on landers or rovers. Orbital measurements can be carried out for bodies whose atmospheres do not greatly attenuate the emitted gamma rays and whose radiation environments do not cause too much background in the detectors. The Moon and Mars, for example, are suitable bodies whereas some of the moons of Jupiter have high backgrounds. In-situ measurements can be passive, relying on the natural radioactivity or cosmic-ray induced reactions, or active, relying on interrogation with manmade radioactive sources or neutron generators.

* Correspondence: Email: cmoss@lanl.gov; Telephone: 505 667 5066; Fax 505 665 3657

Good resolution is much preferred to resolve the many lines expected (Fig. 1). In addition. high efficiency over the range ~0.1 – 10 MeV is required because the counting rate from a planetary body is typically only a few counts per second. The lower limit is determined by the self-absorption in the planetary material, the lack of good lines, and the high background; the upper limit is determine by the Fe(n,γ) lines at 7631, 7645, and 9299 keV. Scintillator detectors, such as NaI(Tl), CsI(Tl), and BGO, provide high efficiency over this range but low resolution. NaI(Tl) detectors were used during the Apollo program[2] and a BGO detector was used for Lunar Prospector.[3] Germanium detectors provide excellent resolution but few have been flown because they require cooling to about 100 K. Germanium detectors were flown on Mars Observer[4] and Mars 96,[5] but both missions failed because of problems unrelated to the detectors.

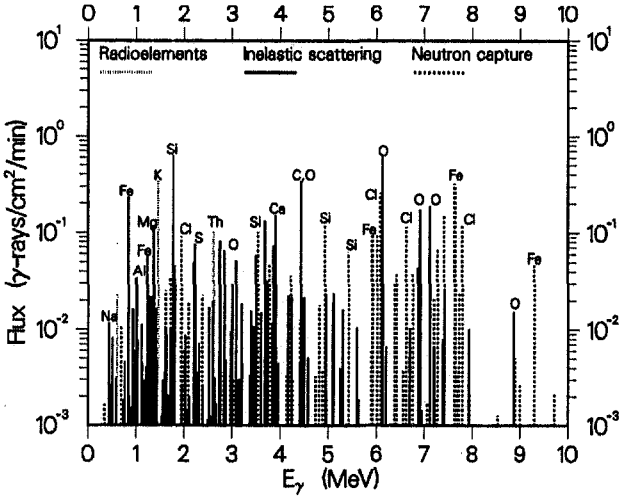

Fig. 1. Calculated gamma-ray lines from Mars at 378 km.[1]

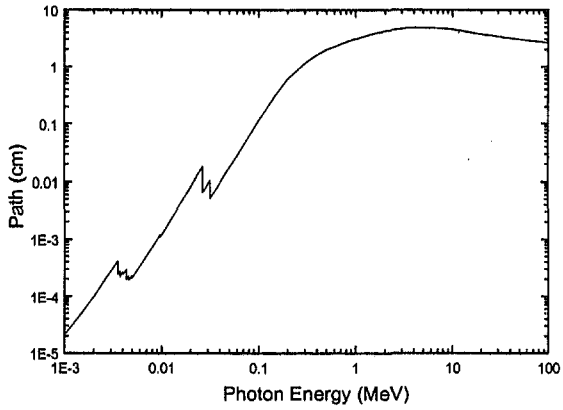

Fig. 2. Calculated mean free path for CdZnTe.[6]

CdZnTe detectors have been manufactured with excellent resolution and peak shape using substrates 15 × 15 × 15 mm^3. Figure 2 shows that the non-coherent mean free path for CdZnTe (mole fraction of zinc, x = 0.2, and density, ρ = 5.86 g/cm^3) has a maximum of 4.9 cm at 5 MeV and hence larger detector volumes are required for studying planetary bodies. The substrate size is currently limited by the growth process, the high-pressure Bridgman process. The material is polycrystalline with nonuniform stoichiometry resulting in grain boundaries and other defects. These defects are often the locations of electron or hole traps that degrade the performance of the detector. Production of spectrometer-grade material with substrate dimensions much greater than 15 × 15 × 15 mm^3 is not expected in the near future.

1.2. Previous techniques to increase efficiency

Achieving good resolution in even this volume detector has required special techniques because of trapping. The trapping length for electrons is usually about 5 cm (at 1000 V/cm) in CdZnTe, but much smaller, typically < 1 mm, for holes. Large-volume, planar detectors with full-area contacts can be manufactured, but the performance is limited by hole tailing. One technique developed by Luke at the Lawrence Berkeley Laboratory for achieving good resolution is the single-polarity charge-sensing method based on a coplanar grid for the anode.[7] An energy resolution of ~1.8% FWHM at 662 keV has been achieved for a cubic cm device.[8]

A second technique involves sensing the interaction depth and electronically compensating for the effects of charge carrier trapping. Methods of sensing the interaction depth include measuring the rise time of each pulse[9] or the ratio of the cathode and the anode signals.[8,10] For planar, full-area contact detectors, the relationship between pulse height and input is accurately modeled by the Hecht relation.[11] Hole tailing can be corrected on a pulse-by-pulse basis if the depth of interaction is known. This approach shows considerable promise and produce results similar to those from coplanar grid detectors. A major benefit of electronic compensation is that a full-area contact can be used. This should result in detectors with consistently lower noise than gridded designs, which can have significant surface leakage between the interdigitated grids. This approach assumes that there is a one-to-one correspondence between the depth of interaction, and hence the correction required. For multiple interactions, which are expected when high-energy gamma rays are detected in large volume detectors, this is not true, and hence a proper correction is not possible. In addition, the complexity of the electronics is increased.

A third technique is the geometrically weighted Frisch grid design proposed by McGregor.[12] The CdZnTe semiconductor is a trapezoid prism with the anode on the small end of the prism and the cathode on the large end. Parallel contacts on the side of the prism form a Frisch grid. The trapezoidal shape allows more interactions to occur in the interaction region over the measurement region than that observed for a parallelepiped parallel strip Frisch grid detector, hence the geometrically weighting. The small area of the anode produces an enhanced response when the electrons move near the anode, the "small pixel" effect.[13,14] This design can be directly connected to a commercially charge sensitive preamplifier without any special summing circuit for grids or rise-time circuit. One disadvantage is the relatively low photopeak efficiency.

The efficiency, or active volume, CdZnTe detectors have been modelled.[15] Three cases were considered: a conventional planar detector, a unipolar device, and a detector in which electronic signal processing is applied to correct for charge trapping. The active volume is different from the physical volume of a detector because of trapping effects. The study found that the active thickness of commercially available planar detectors is limited to about 2 mm, and of unipolar devices, to about 5 mm. The study concludes that the most promising approach for attaining a large volume (> 1 cm^3) in a single detector is with a unipolar device using some form of electronic compensation for electron trapping. The disadvantages of electronic compensation were noted above.

A fourth technique is to use a stacked array of single CdZnTe detector elements and sum the signals, either with analog or digital circuits. Results from the summing of the analog signals from up to three planar detectors before the preamplifier have been reported.[16] The detectors are matched by adding a simple RC network to the detectors with the highest outputs to discard a fraction of the charge. The spectra showed considerable hole tailing because they were not unipolar devices. The main advantage of this approach is its simplicity. A disadvantage is the increased leakage current and capacitance, which lead to increased system noise and degraded energy resolution for a large (>3 detectors) array.

2. PROPOSED DESIGN

The approach described in the present report involves a three-dimensional array of single CdZnTe detector elements to achieve both good resolution and moderate efficiency at ambient temperature for MeV gamma rays. We propose a $3 \times 3 \times 3$ array of $15 \times 15 \times 15$ mm^3 detectors, a "Rubic's" cube, which will provide a cubic volume of $45 \times 45 \times 45$ mm^3. Detectors $15 \times 15 \times 15$ mm^3 volume have been produced commercially, and the dimension of 4.5 cm is consistent with the mean free path of 4.9 cm noted above. Each detector will be designed for optimal performance by using the best available electrode design and surface passivation to reduce surface leakage. The detector design currently favored and used for the results discussed below has a coplanar grid.

We propose to package the detectors in individual thin-wall boxes. Figure 3 shows a stack of three such boxes, which have been fabricated. The detectors are mounted on alumina, which is the standard material for mounting, but each piece of alumina is only slightly larger than the area of the detector. Traditionally, the area of the alumina has been much oversize to accommodate the mounting of pins for attaching bond wires and to facilitate the handling of the detector. The sides and top

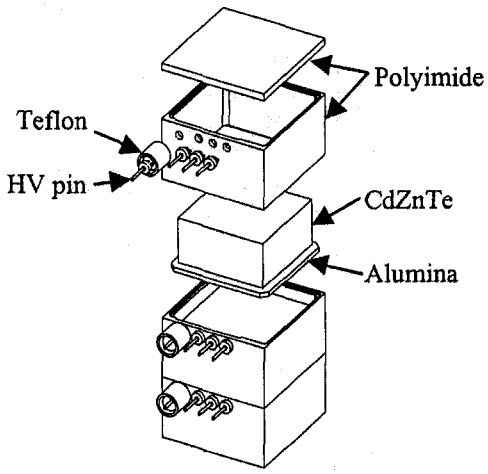

Fig. 3. Stack of boxes for three CdZnTe detectors.

of the box are polyimide, which is much more easily fabricated and mechanically less fragile but an excellent insulator, sometimes used for printed circuit boards. Stacks of detectors can be clustered together to form a three-dimensional array. This design allows the detectors to be closely packed to reduce the loss of efficiency for multi-detector events. It also facilitates handling and replacement of individual detectors. The HV is applied to the pin in the teflon insulator and the other three pins provide connections to the two grid electrodes in the coplanar grid and ground. Preamplifier boards with matching sockets are plugged onto these pins. For arrays larger than $2 \times 2 \times 2$ the boxes for the interior detectors will not have these types to pins but rather the connections will be made with kapton flex cable. The disadvantage of using boxes is the absorption of gamma rays in the box walls, which can reduce the overall photopeak efficiency of the array.

The signals from the two grids on each detector are combined in a difference circuit located on the preamplifier board to produce a single signal for each detector. These coincident signals, in turn, are combined in software or hardware to produce a spectrum equivalent to one from a detector with a larger volume than the volume of any one detector. In order to avoid excessive noise, which is a potential problem in technique four above, only detector signals that exceed a threshold are combined. We are investigating several digital signal processors to digitize the difference signals as well as several analog approaches. The analog approaches might require less power, which is very important for space missions. Note that enough flexibility is required for a space mission so that, for example, specific detectors can be disabled, the outer elements in the array can be used to reject charged particles or other backgrounds, or the signals can be processed to produce full-energy, single-escape, or double-escape spectra. These tasks might be more easily performed with digital circuitry. The preliminary results reported below were obtained with analog circuitry.

3. PREDICTED RESULTS

We have developed extensive capabilities to model the radiation transport, the electric fields inside the crystals, and the charge transport. The agreement between calculations and experiments is excellent.[17] Figure 4 shows the calculated response of a $3 \times 3 \times 3$ array of $15 \times 15 \times 15$ mm^3 coplanar-grid detectors based on the measured parameters of one detector. The suppressed spectrum is generated by requiring coincidence in two or more detectors and summing the response. This procedure shifts some of the counts from the Compton continuum to the full-energy peaks, thus suppressing the Compton continuum. The well-defined peaks, especially at high energy, are adequate for determining the elemental compositions of planetary bodies. In particular, note the peak at 7.6 MeV for iron.

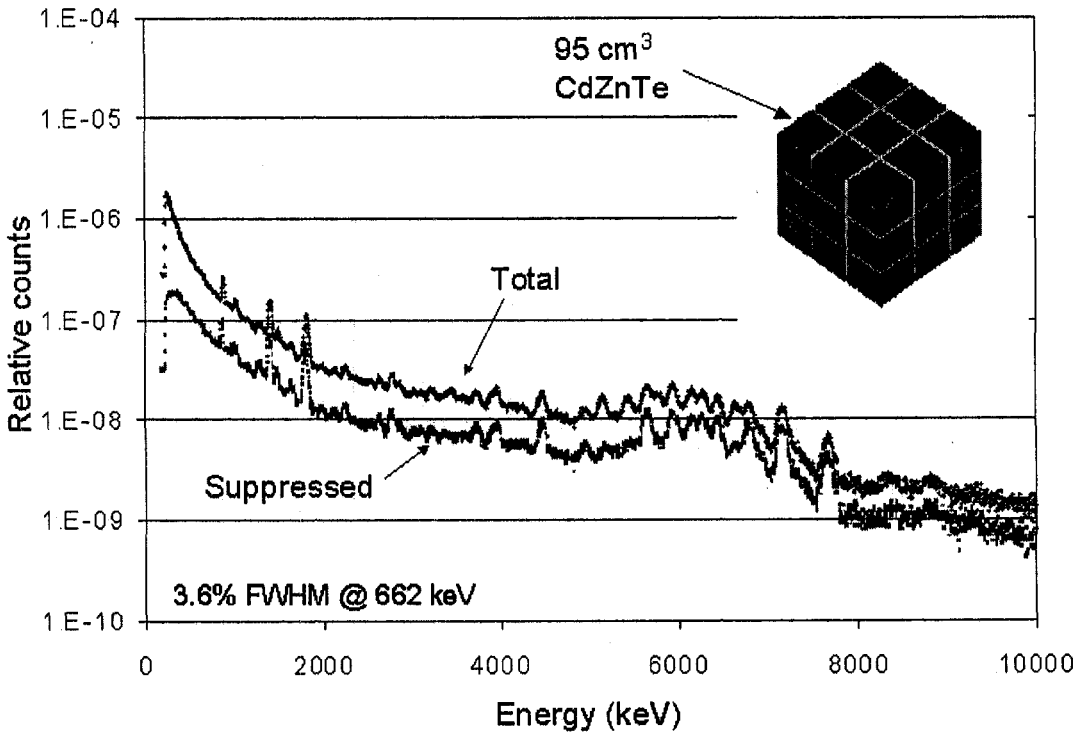

Fig. 4. Calculated lunar highlands spectrum for a 27-detector CdZnTe gamma-ray spectrometer.

4. EXPERIMENTAL DETAILS

4.1. Detectors

We have used the detectors listed in Table 1 to study the physics and electronics for a three-dimensional array. These

Table 1. Parameters of detectors used for preliminary results.

Detector Type	Supplier	Serial Number	Dimensions (mm)	Bias (V)	Resolution FWHM (%)[a]
Cube, coplanar	eV Products	2058	15 × 15 × 15	-2400	3.2
Parallelepiped, coplanar	eV Products	I315201	15 × 15 × 8	-1500	3.0
Cube, coplanar	LBNL	1761-01	10 × 10 × 10	-1400	3.3
Cube, coplanar	LBNL	176102	10 × 10 × 10	-1400	2.4
Cylinder, radial coplanar	eV Products	C26-02	10 (dia) × 5	-1200	4.1
Cylinder, radial coplanar	eV Products	C26-05	10 (dia) × 5	-1500	1.8
Cylinder, radial coplanar	eV Products	C26-14	10 (dia) × 5	-1000	2.7
Cylinder, radial coplanar	eV Products	I03-01	10 (dia) × 5	-1000	2.2
Cylinder, radial coplanar	eV Products	I03-02	10 (dia) × 5	-800	1.9
Cylinder, radial coplanar	eV Products	I03-06	10 (dia) × 5	-1200	2.4

a) At 662 keV

detectors were used because larger detectors for the array were not available yet. Even these detectors were not always available because they were needed for other projects. Using a small number of detectors reduces the complexity of the setup.

4.2. Electronics

A typical circuit for the coincident measurement with two detectors is shown in Fig. 5. The difference circuit and bias between the anode grids was optimized for the best resolution at 662 keV; grid biases were in the range -30 to -100 V. The shaping amplifiers, gate delays, linear gates, and sum amplifier were all NIM modules. Stretched (i.e., approximately

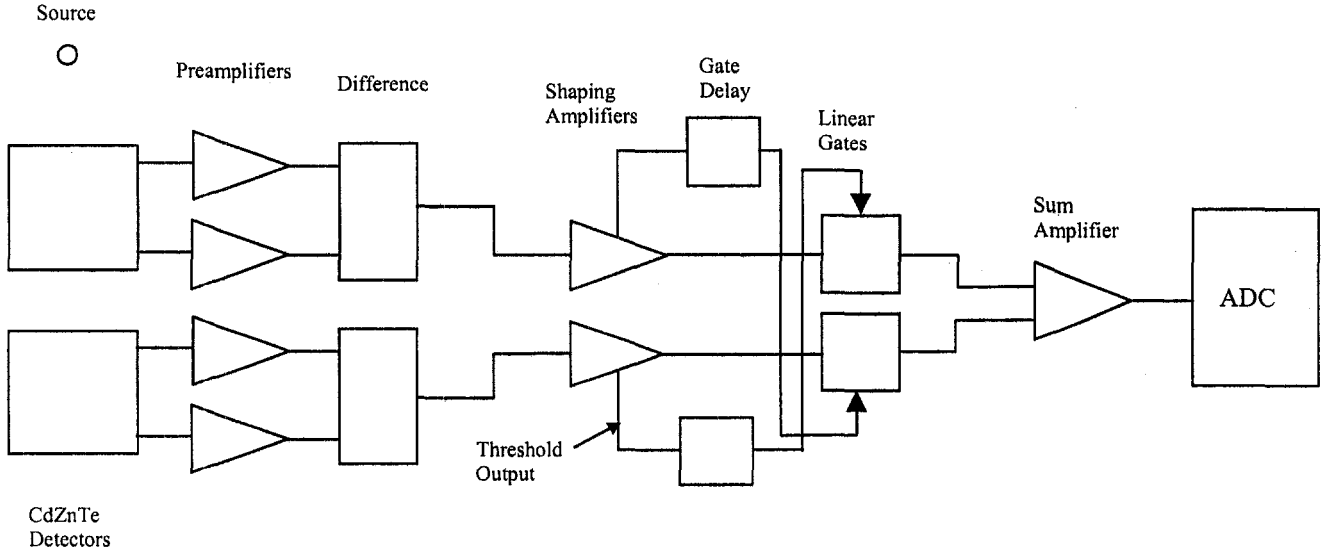

Fig. 5. Block diagram of the electronics used for the two-detector coincidence measurements.

rectangular) pulses 3 μs long from the shaping amplifiers were used for to accommodate the time jitter of ≤1 μs from the detectors, probably caused by charge collection in the detectors. The shaping amplifiers contained an adjustable threshold that generated a gate whenever a pulse exceeded the set value, except for pile-up pulses. The circuit is normally used for pile-up rejection and associated dead time correction. These gates were delayed and increased to slightly greater than 3 μs for the gate enable inputs to the linear gates. The maximum amplitude of the output from the sum amplifier was correct and was correctly processed by the ADC even if the pulses from the two detectors arrived at slightly different times.

Several requirements must be met to obtain good results with this technique. The droop of the stretched output from the shaping amplifiers must be small and the DC offsets and linearity of all of the modules must be good. We were able to find commercial modules meeting these requirements. The counting rates in each detector must be limited, say ≤1 kHz, to avoid pileup and chance coincidences caused by the use of long pulses.

The circuit for more than two detectors is based on a commercial ≥ n-fold coincidence circuit. The output of this circuit is fed to coincidence circuits for each threshold gate and the output of these individual coincidence circuits used to open the linear gates.

5. RESULTS

5.1. 15 × 15 × 15 mm^3 detector

Figure 6 shows results for a single 15 × 15 × 15 mm^3 detector, the baseline detector size for our array design. The spectra show the response to a range of energies (keV): ^{137}Cs, 662; ^{60}Co, 1332; ^{228}Th, 2614; and ^{244}Cm/^{13}C, 6129. The ^{244}Cm/^{13}C source produces the 6129-keV gamma rays by the reaction ^{13}C(α,nγ)^{16}O, where the alpha particles are produced by the decay of ^{244}Cm. At 662 keV the height of the photopeak greatly exceeds the height of Compton continuum, at 1332 and 2614 keV the heights are comparable, and at 6129 keV the Compton continuum is dominant. These results indicate that at higher energies Compton suppression might be required even in detectors as large as 15 × 15 × 15 mm^3.

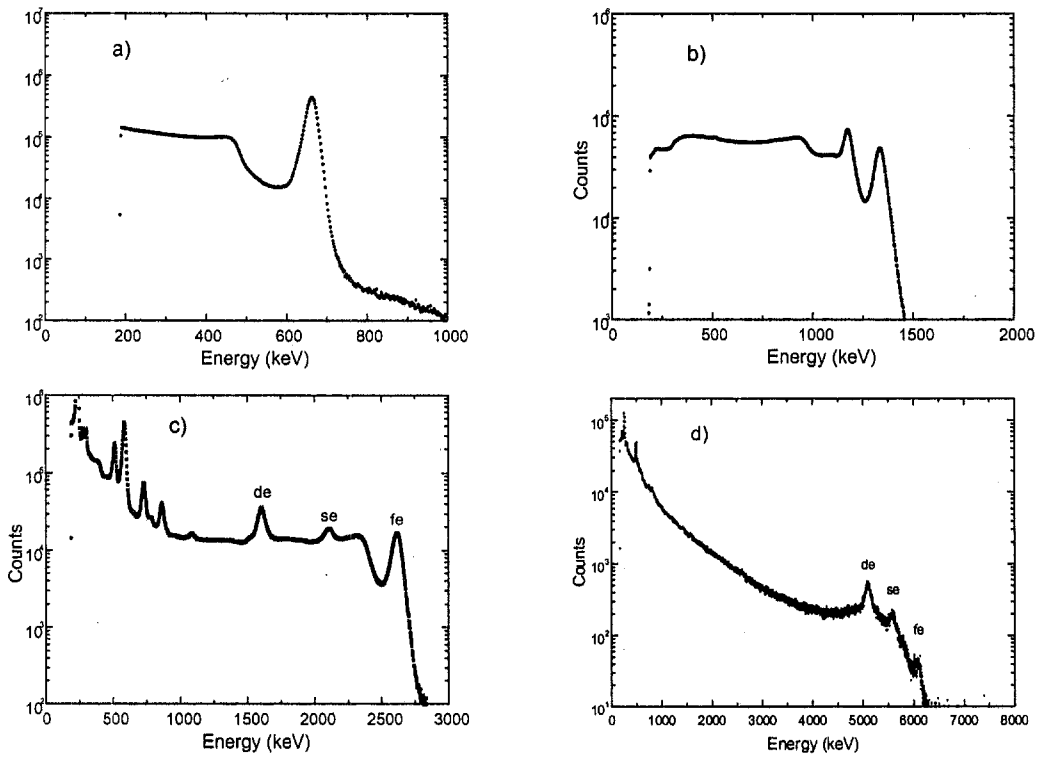

Fig. 6. Spectra from a single 15 × 15 × 15 mm^3 detector. a) ^{137}Cs, b) ^{60}Co, c) ^{228}Th, and d) ^{244}Cm/^{13}C.

5.2. Cylindrical detectors

Results for two cylindrical detectors (10mm(diameter) × 5mm(thickness)) are shown in Fig. 7. The detectors were stacked with the anodes about 2 mm apart, which was the closest we could safely place them with their existing mounting, but this was close enough to give adequate counting rates of coincident events. For the single detector measurement of ^{60}Co (Fig. 7a), the signal still was sent through the linear gate but the gate was derived from the threshold gate for that detector. Note the large reduction in the Compton continuum in the ^{60}Co spectrum produced by requiring coincidence (Fig. 7b). The counting rate in the 1332-keV peak dropped from 2.1 to 0.5 counts/s while the FWHM increased from 4.3 to 4.6%. The resolution of both measurements is probably degraded with respect to the manufacturer's reported results by the increase

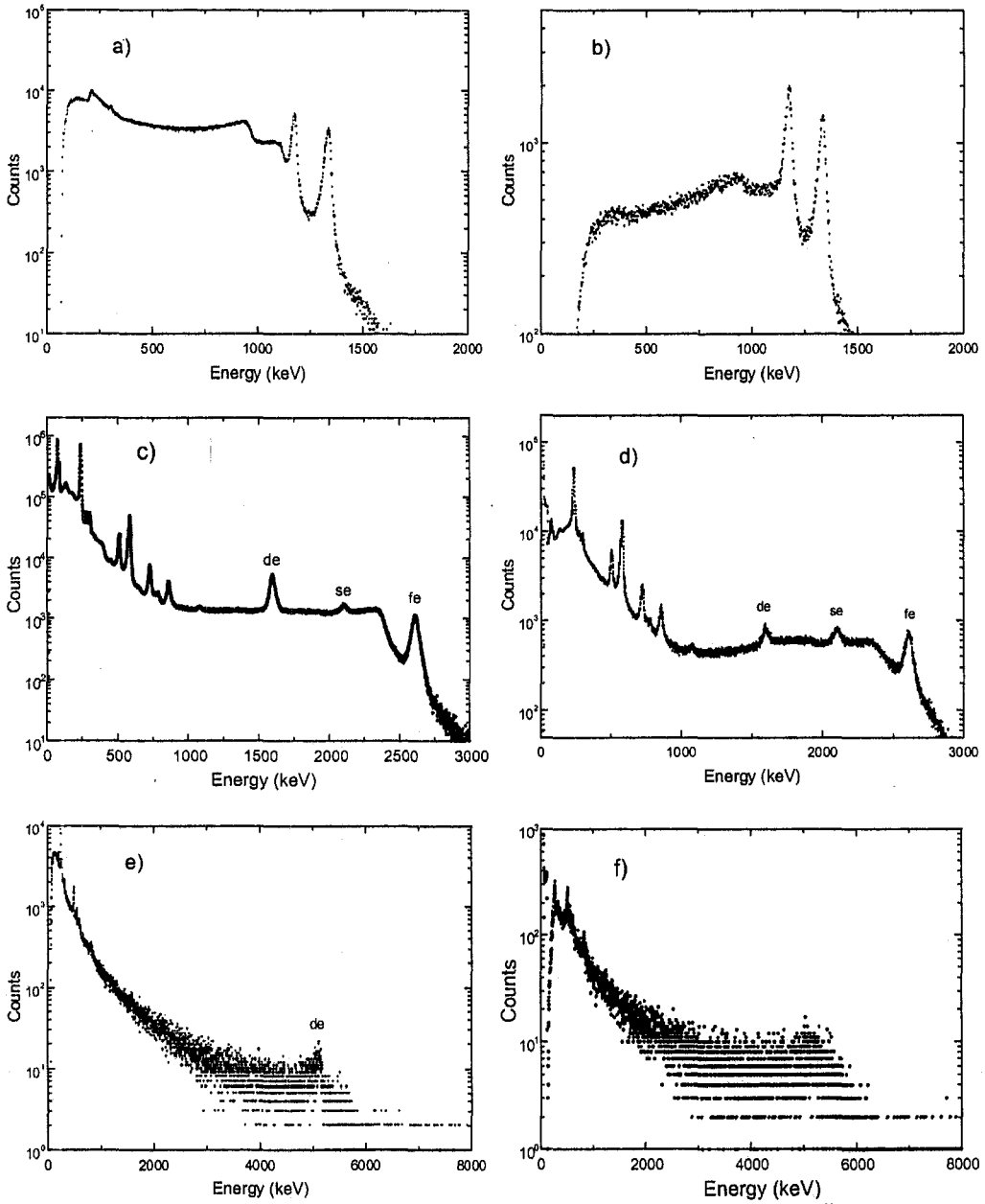

Fig. 7. Cylindrical detector spectra. a) Single detector spectrum of ^{60}Co. b) Coincidence spectrum of ^{60}Co. c) Summed spectrum without coincidence of ^{228}Th. d) Coincidence spectrum of ^{228}Th. e) Single detector spectrum of ^{244}Cm/^{13}C. f) Coincidence spectrum of ^{244}Cm/^{13}C.

in length of the wires connecting each detector to its preamplifier for this stacking configuration and by the linear gate on each detector.

Similar results were obtained for ^{228}Th. Fig. 7c shows a summed spectrum measurement in which each detector was gated by the gate derived from its threshold gate and the linear signals were summed by the sum amplifier. The counting rate is approximately twice the rate in a single detector, except at low energy where the front detector attenuates the gamma rays significantly before they reach the back detector. Requiring coincidence (Fig. 7d) does not reduce the Compton continuum from the 2614-keV gamma ray as much as it did for the 1332-keV gamma ray from ^{60}Co. However, note the large reduction in the second escape peak. The counting rate in the 2614-keV peak dropped from 4.7 in the summed spectrum to 0.7 counts/s in the coincidence spectrum while the FWHM increased from 1.8 to 1.9 %.

Similar measurements were attempted for the ^{244}Cm/^{13}C source with these small cylindrical detectors. A single detector spectrum gated by its own gate spectrum (Fig. 7e) and coincidence spectrum (Fig. 7f) are shown. The counts rate in a region of interest including the full energy, single escape, and double peaks are 0.038 and 0.027 counts/s, respectively. The low rate is attributed to the low emission rate of the source, the low cross section for interaction at this higher energy, and the small size of the detectors. Note, however, the large number of lower-energy photons in the Compton continuum, which could be detected and summed into the photopeak with a large array of larger detectors.

5.3. $10 \times 10 \times 10$ mm^3 detectors

We also made many measurements with two $10 \times 10 \times 10$ mm^3 detectors. The detectors, packaged in plastic cylinders with a tungsten back shield on the cathode side, were placed side by side with a gap of about 19 mm between the active volumes. The gamma rays from the various sources were incident on the side.

Some of the physics of the interactions in these two cubic detectors is clearer in spectra taken with ^{137}Cs, which has a single moderately high-energy line at 662 keV. The Compton continuum and the backscatter peaks are clearly visible in the linear plots of the single detector spectra gated by their respective threshold gates (Figs. 8a and b). The Compton continuum and the backscatter peak are greatly reduced in the coincidence spectrum (Fig. 8c). For the front, back, and coincidence spectra, respectively, the photopeak counting rate (counts/s) and FWHM are: 20.1, 3.7 %; 5.1, 2.7 %; and 0.094, 3.6 %. The much lower counting rate in the coincidence spectrum is caused by the 19-mm gap between the active volumes.

We have also measured the contribution of each detector to the coincidence spectrum (Figs. 8d and e). The Compton peak in the back detector (Fig. 8e) is probably produced by a gamma ray that penetrates trough the first detector and undergoes a 180-degree Compton scattering. The resulting low-energy gamma ray then interacts in the front detector to produce the backscatter peak (Fig. 8d). These features are expected to shift in energy if the geometry, and therefore the scattering angles, are changed.

These cubic detectors offer performance that is intermediate between that of $15 \times 15 \times 15$ mm^3 cubic detectors and the cylindrical detectors, as expected, because their volume is also intermediate. At 6129 keV a single detector gives clearly visible full energy, single escape, and double escape peaks (Fig. 9a) whereas these peaks are not apparent in the coincidence spectrum with a live time of 123036 s (Fig. 9b). For the single detector the counting rate in the 6129-keV full-energy peak was 0.0069 counts/s and the FWHM was 1.3 %.

5.4. More than two detectors

We also made attempts to measure spectra with more than two detectors using a 2-fold coincidence circuit. As mentioned above, the current mounting substrates prevented more than two detectors from being placed close together and thus the possible efficiency was too low to yield useful results. In addition, the complexity of the electronics makes setting up NIM electronics difficult with low counting rates.

6. CONCLUSIONS

Our results for several combinations of smaller detectors operating in coincidence as well as for a single $15 \times 15 \times 15$ mm^3 detector indicate that our approach to achieving good efficiency by combining the signals from a three-dimensional array of large detectors will work. Good efficiency and a spectrum not complicated by a large Compton continuum can be achieved

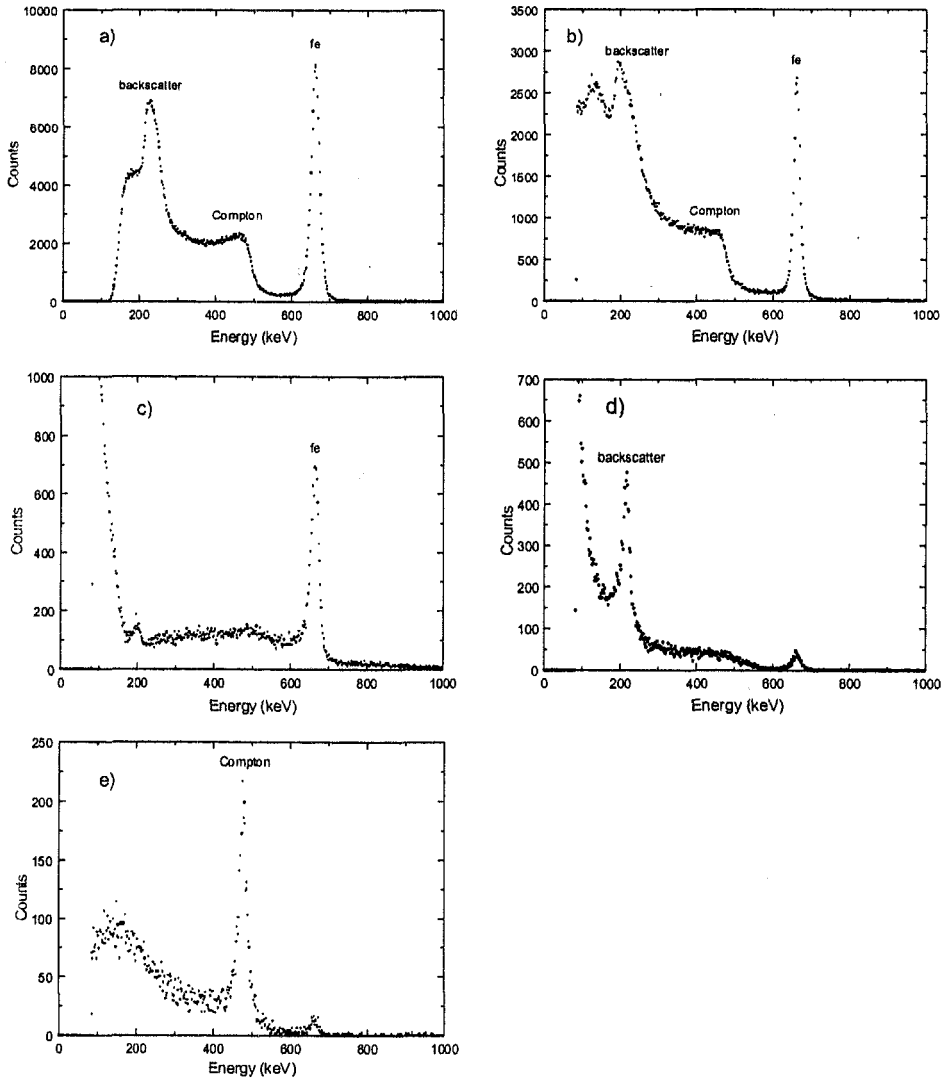

Fig. 8. Cubic detector spectra of ^{137}Cs. a) Spectrum from the front detector without coincidence. b) Spectrum from the back detector without coincidence. c) Coincidence spectrum. d) Spectrum from the front detector in coincidence with the back detector. e) Spectrum from the back detector in coincidence with the front detector.

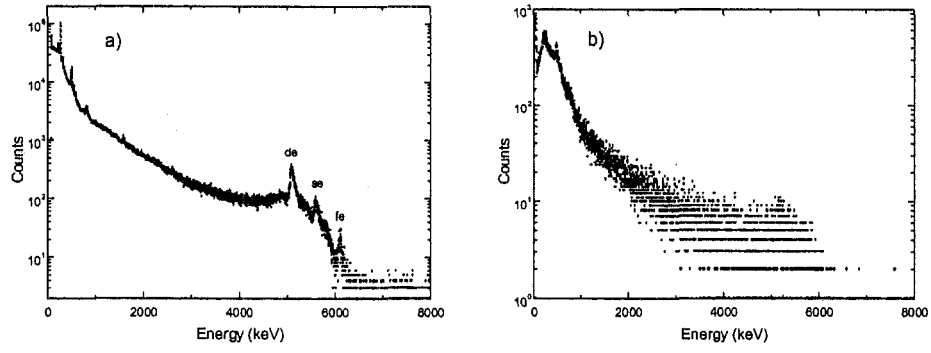

Fig. 9. Cubic detector spectra of $^{244}Cm/^{13}C$. a) Single detector spectrum. b) Coincidence spectrum.

by simply summing the spectra from 15 × 15 × 15 mm^3 detectors for gamma-ray energies below about 2 MeV. Above 2 MeV, 2-fold coincidence might be required, depending on the spectrum, to suppress the Compton continuum and escape peaks. Electronics that can operate in these two modes to accurately combine the signals from the individual detectors as well as provide more detailed information for diagnostics are required.

ACKNOWLEDGEMENTS

Phyllis Russo and Bill Murray loaned us some of the detectors. Chris Romero designed the detector boxes, and Lawrence Garcia and Manuel Baca fabricated them. The work was supported by NASA's Planetary Instrument Definition and Development Program and done under the auspices of the US DOE.

REFERENCES

1. J. Masarik and R.C.Reedy, "Gamma Ray Production and Transport in Mars," J. *Geophys. Res.* **101**, pp. 18,891-18,912, 1996.
2. T.M. Harrington, J.H. Marshall, J.R. Arnold, L.E. Peterson, J.I.Trombka, and A.E. Metzger, "The Apollo gamma-ray spectrometer." *Nucl. Instr.and Meth.* **118**, pp. 401-411, 1974.
3. W.C. Feldman, B.L. Barraclough, K.R. Fuller, D.J. Lawrence, S. Maurice, M.C. Miller, T.H. Prettyman, and A.B. Binder, "The Lunar Prospector gamma-ray and neutron spectrometers," *Nucl. Instr. and Meth.* **A 422**, pp. 562-566, 1999.
4. W.V. Boynton, J.I. Trombka, W.C. Feldman, J.R. Arnold, P.A.J. Englert, A.E. Metzger, R.C. Reedy, S. W. Squyres, H. Waenke, S.H. Bailey, J. Brueckner, J.L. Callas, D.M. Drake, P. Duke, L.G. Evans, E.L. Haines, F.C. McCloskey, H. Mills, C. Shinohara, and R. Starr, "Science Applications of the Mars Observer Gamma Ray Spectrometer," *J. Geophys. Res.* **97**, pp. 7681-7698, 1992.
5. G. Mitrofanov, D.S. Anfimov, A.M. Chernenko, V.Sh. Dolidze, V.I.Kostenko, O.E. Isupov, A.S. Pozanenko, A.K. Ton'shev, D.A. Ushakov, Yu.I. Bobrovnitsky, T.M. Tomilina, G.F. Auchampaugh, M.M. Cafferty, D.M. Drake, E.E. Fenimore, R.W. Klebesadel, J.L. Longmire, C.E. Moss, R.C.Reedy, and J.E. Valencia, "Germanium Gamma-Ray Spectrometer PGS for the MARS-96 Mission," *SPIE* **2808**, pp. 595-604, 1996.
6. M.J. Berger and J.H. Hubbell, *XCOM: Photon Cross Sections Database*, National Institute of Standards and Technology Standard Reference Database 8 (XGAM), NBSIR 87-3597 (1998).
7. P.N. Luke, "Unipolar charge sensing with coplanar electrodes—application to semiconductor detectors," *IEEE Trans. Nucl. Sci.* **42** (4), pp. 207-213, 1995.
8. Z. He, G.F. Knoll, D.K. Wehe, and J. Miyamoto, "Position-sensitive single carrier CdZnTe detectors," *Nucl. Instr. and Meth.* **A 388**, pp. 180-185, 1997.
9. M. Richter and P. Siffert, "High resolution gamma ray spectroscopy with CdTe detector systems," *Nucl. Instr. and Meth.* **A322**, pp. 529-537, 1992.
10. Z. He, G.F. Knoll, D.K. Wehe, R. Rojeski, C.H. Mastrangelo, M. Hammig, C. Barrett, and A. Uritani, "1-d position sensitive single carrier semiconductor detectors," *Nucl. Instr. and Meth.* **A 380**, pp. 228-231, 1996.
11. K. Hecht, "Zum mechanismus des lichtelektrischen primarstromes in isolierenden kristallen," *Z. Physik* **77**, pp. 235-245, 1932.
12. D.S. McGregor, R.A. Rojeski, Z. He, D.K. Wehe, M. Driver, and M. Blakely, " Geometrically weighted semiconductor Frisch grid radiation spectrometers," *Nucl. Instr. and Meth.* **A 422**, pp. 164-168, 1999.
13. H.H. Barrett, J.D. Eskin, and H.B. Barber, "Charge transport in arrays of semiconductor gamma-ray detectors," *Phys. Rev. Lett.* **75**, pp. 156-159, 1995.
14. W. Shockley. "Currents to conductors induced by a moving point charge," *J. Appl. Phys.* **9**, pp. 635-636 , 1938.
15. J.C. Lund, B.A. Brunett, T.P. Viles, N.R. Hilton, and R.B. James, "On the active volume of cadmium zinc telluride gamma-ray spectrometers," *Mat. Res. Soc. Symp. Proc.* **487**, pp. 199-204, 1998.
16. R. Olsen, R.B. James, A.J. Antolak, and C. Wang, "Development of high-resolution cadmium zinc telluride and mercuric iodide gamma-ray detectors for use in non-proliferation," *Proceedings of the 35th Annual Meeting of the Institute of Nuclear Materials Management* **23**, p. 589-604, 1994.
17. T.H. Prettyman, C.S. Cooper, P.N. Luke, P.A. Russo, M. Amman, and D.J. Mercer, "Physics-based generation of gamma-ray response functions for CdZnTe detectors," *J. Radioanal. Nucl. Chem.* **233**, pp. 257-264, 1998.